A FDTD ALGORITHM FOR THE ANALYSIS OF SHORT OPTICAL PULSE SECOND HARMONIC GENERATION IN DISPERSIVE MEDIA

M. A. Alsunaidi, F. S. Alhajiri, and H. M. Masoudi
Department of Electrical Engineering, King Fahd University of Petroleum and Minerals, PO Box 200 Dhahran 31261, Saudi Arabia; Corresponding author: msunaidi@kfupm.edu.sa

ABSTRACT: *A time-domain nonlinear model representing the propagation of ultra-short optical pulses in dispersive materials containing second order nonlinearity is presented. The model accounts for material dispersion through Lorentz model in addition to the spatiotemporal coupling between the pulsed fundamental and second harmonic beams. Numerical results for the generated second harmonic pulse clearly demonstrate the pulse break-up phenomenon.* © 2009 Wiley Periodicals, Inc. Microwave Opt Technol Lett 51: 1097–1100, 2009; Published online in Wiley InterScience (www.interscience.wiley.com). DOI 10.1002/mop. 24213

1. INTRODUCTION

Time-domain analysis of nonlinear effects in modern optical devices provides an invaluable insight into the understanding and potential utilization of device behavior and wave-device interaction. On the other hand, the increased progress in materials technology and fabrication methods for integrated optics has resulted in a growing need for accurate models that closely predict the behavior of the electromagnetic fields inside new optical devices. The process of nonlinear optical Second Harmonic Generation (SHG) has been extensively studied in literature with growing interest. For CW inputs or long pump pulses, it is quite sufficient to match the phase velocities of the propagating beams for optimum conversion [1]. As the bandwidth of the pump pulse increases, the group velocity mismatch and wave packet spreading need to be taken into consideration [2]. These effects become significant for pulse durations of less than 100 femtoseconds. The reported attempts to model and simulate pulsed SHG in dispersive second order materials involved 1-D approximations with high-order time derivatives and input depletion ignored (for example, Ref. 3, 4) to simplify the analysis.

In this article, the analysis of ultrashort optical pulse propagation in second order nonlinear material is introduced. The model is an extension of the work in Ref. 5, wherein CW inputs were considered. The formulation of the problem involves incorporating the frequency-dependent material dispersion in the time-domain SHG model. Next, explicit, uncoupled FDTD solution equations are obtained. The present model fully accounts for all temporal and spatial variations and takes the depletion of the input beam into consideration.

2. FORMULATIONS

The coupled nonlinear equations representing the propagating fundamental input, f, and the generated second harmonic field, s, inside a second order nonlinear optical structure are given by the following nonlinear wave equations [5]

$$\nabla^2 f = \mu_o \varepsilon_o \varepsilon_r^f \frac{\partial^2 f}{\partial t^2} + \mu_o \varepsilon_o \chi^{(2)}(\omega) \frac{\partial^2}{\partial t^2}(fs) \quad (1)$$

$$\nabla^2 s = \mu_o \varepsilon_o \varepsilon_r^s \frac{\partial^2 s}{\partial t^2} + \mu_o \varepsilon_o \chi^{(2)}(2\omega) \frac{\partial^2}{\partial t^2}(f^2) \quad (2)$$

where, ε_r is the material dielectric constant and $\chi^{(2)}$ is the dispersionless nonlinear susceptibility. The application of the FDTD algorithm prescribed by Eqs. (1) and (2) for modeling CW-SHG processes in nonlinear optical devices has been demonstrated in an earlier publication [5]. Being a time-domain model, it was noted there, however, that the model had a great potential in the analysis of short-pulse propagation. To achieve this task, adequate representation of the frequency-dependent material parameters of the optical device need to be employed. In particular, material dispersion at optical frequencies has to be included in the model. The frequency-dependent dispersion relation of the dielectric constant is best represented by the Lorentz equation

$$\varepsilon_r(\omega) = \varepsilon_\infty + \frac{(\varepsilon_s - \varepsilon_\infty)\omega_o^2}{\omega_o^2 + 2j\omega\delta - (j\omega)^2} \quad (3)$$

where, ε_s and ε_∞ are the static and optical values of the dielectric constant, respectively, ω_0 is the material resonance frequency and δ is the damping factor. The frequency dependence in the dispersion relation is accommodated in the time domain model through an auxiliary differential equation relating the electric flux density, D, to the field intensity. The Auxiliary Differential Equation (ADE) approach is discussed in Ref. 6.

For the fundamental wave, the frequency domain equation for the electric flux density is given by the following equation

$$D^f(\omega) = \varepsilon_o \varepsilon_r(\omega) f(\omega) + \varepsilon_o \chi^{(2)}(fs)(\omega) \quad (4)$$

where, the second term in the right hand side represents the contribution of the second order nonlinear polarization. Using Eq. (3), Eq. (4) becomes the following

$$\omega_o^2 D^f + 2\delta(j\omega)D^f + (j\omega)^2 D^f = \varepsilon_o \varepsilon_s \omega_o^2 f + 2\varepsilon_o \varepsilon_\infty \delta(j\omega)f$$
$$+ \varepsilon_o \varepsilon_\infty (j\omega)^2 f + \varepsilon_o \chi^{(2)} \omega_o^2 fs + 2\varepsilon_o \chi^{(2)} \delta(j\omega) fs + \varepsilon_o \chi^{(2)}(j\omega)^2 fs \quad (5)$$

Taking the inverse Fourier transform of Eq. (5), the following time-domain differential equation is obtained.

$$\omega_o^2 D^f + 2\delta \frac{\partial D^f}{\partial t} + \frac{\partial^2 D^f}{\partial t^2} = 2\varepsilon_o \varepsilon_\infty \delta \frac{\partial f}{\partial t} + \varepsilon_o \varepsilon_\infty \frac{\partial^2 f}{\partial t^2} + \varepsilon_o \varepsilon_s \omega_o^2 f$$
$$+ \varepsilon_o \chi^{(2)} \omega_o^2 fs + 2\epsilon_o \chi^{(2)} \delta \frac{\partial(fs)}{\partial t} + \varepsilon_o \chi^{(2)} \frac{\partial^2(fs)}{\partial t^2} \quad (6)$$

Similarly, for the second harmonic wave, with

$$D^s(\omega) = \varepsilon_o \varepsilon_r(\omega) s(\omega) + \varepsilon_o \chi^{(2)} f^2(\omega) \quad (7)$$

it can be shown that

$$\omega_o^2 D^s + 2\delta \frac{\partial D^s}{\partial t} + \frac{\partial^2 D^s}{\partial t^2} = 2\varepsilon_o \varepsilon_\infty \delta \frac{\partial s}{\partial t} + \varepsilon_o \varepsilon_\infty \frac{\partial^2 s}{\partial t^2} + \varepsilon_o \varepsilon_s \omega_o^2 s$$
$$+ \varepsilon_o \chi^{(2)} \omega_o^2 f^2 + 2\varepsilon_o \chi^{(2)} \delta \frac{\partial f^2}{\partial t} + \varepsilon_o \chi^{(2)} \frac{\partial^2 f^2}{\partial t^2} \quad (8)$$

The fundamental and second harmonic flux densities are related to the electric field intensities, respectively, by as follows

$$\frac{\partial^2 D^f}{\partial t^2} = \frac{1}{\mu_o}\nabla^2 f \tag{9}$$

$$\frac{\partial^2 D^s}{\partial t^2} = \frac{1}{\mu_o}\nabla^2 s \tag{10}$$

The resulting dispersive SHG model equations are strongly-coupled highly-nonlinear set of partial differential equations. These equations provide a time-dependent self-consistent solution for the propagation of the input wave as well as the subsequent generation of the second harmonic wave for any input conditions. Considering the sensitivity of the SHG problem to phase differences between the propagating waves, the equations need to be solved in their complete form. In particular, for nonparaxial and short pulse time profiles, high-order time derivatives play an important role. Hence, slowly varying envelop (SVE) approximations cannot be used.

3. DECOUPLED NL-FDTD SOLUTION

The derivations above result in a strongly-coupled highly-nonlinear set of partial differential equations. To decouple these equations, a common practice in CW and SVE operations is to drop the time derivatives of the second harmonic field in Eq. (8), as in Ref. 5. The underlying assumption in this case is that first and second derivatives contribute insignificantly to the power coupling phenomenon. For short-pulse operations in dispersive media, the phase calculations are affected immensely by the time derivatives. Hence, the equations ought to be solved in their entirety. Starting with the second harmonic field, the derivatives in Eq. (8) are approximated by FDTD central differences at time level n as following

$$\frac{\omega_o^2}{2}(D^{s(n+1)} + D^{s(n-1)}) + \frac{2\delta}{2\Delta t}(D^{s(n+1)} - D^{s(n-1)})$$

$$+ \frac{1}{\Delta t^2}(D^{s(n+1)} - 2D^{sn} + D^{s(n-1)}) = \frac{2\varepsilon_o\varepsilon_\infty\delta}{2\Delta t}(s^{n+1} - s^{n-1})$$

$$+ \frac{\varepsilon_o\chi^{(2)}\omega_o^2}{2}(f^{2(n+1)} + f^{2(n-1)}) + \frac{\varepsilon_o\chi^{(2)}}{\Delta t^2}(f^{2(n+1)} - 2f^{2n} + f^{2(n-1)})$$

$$+ \frac{\varepsilon_o\varepsilon_\infty}{\Delta t^2}(s^{n+1} - 2s^n + s^{n-1}) + \frac{\varepsilon_o\varepsilon_s\omega_o^2}{2}(s^{n+1} + s^{n-1})$$

$$+ \frac{2\varepsilon_o\chi^{(2)}\delta}{2\Delta t}(f^{2(n+1)} - f^{2(n-1)}) \tag{11}$$

Solving for $s^{(n+1)}$, we get as follows

$$s^{(n+1)} = D^{s(n+1)}\frac{\left(\dfrac{\omega_o^2}{2} + \dfrac{\delta}{\Delta t} + \dfrac{1}{\Delta t^2}\right)}{\left(\dfrac{\varepsilon_o\varepsilon_\infty\delta}{\Delta t} + \dfrac{\varepsilon_o\varepsilon_\infty}{\Delta t^2} + \dfrac{\varepsilon_o\varepsilon_s\omega_o^2}{2}\right)}$$

$$+ D^{s(n-1)}\frac{\left(\dfrac{\omega_o^2}{2} - \dfrac{\delta}{\Delta t} + \dfrac{1}{\Delta t^2}\right)}{\left(\dfrac{\varepsilon_o\varepsilon_\infty\delta}{\Delta t} + \dfrac{\varepsilon_o\varepsilon_\infty}{\Delta t^2} + \dfrac{\varepsilon_o\varepsilon_s\omega_o^2}{2}\right)} +$$

$$+ D^{sn}\frac{\left(\dfrac{-2}{\Delta t^2}\right)}{\left(\dfrac{\varepsilon_o\varepsilon_\infty\delta}{\Delta t} + \dfrac{\varepsilon_o\varepsilon_\infty}{\Delta t^2} + \dfrac{\varepsilon_o\varepsilon_s\omega_o^2}{2}\right)} + s^{n-1}\frac{\left(\dfrac{\varepsilon_o\varepsilon_\infty\delta}{\Delta t} - \dfrac{\varepsilon_o\varepsilon_\infty}{\Delta t^2} - \dfrac{\varepsilon_o\varepsilon_s\omega_o^2}{2}\right)}{\left(\dfrac{\varepsilon_o\varepsilon_\infty\delta}{\Delta t} + \dfrac{\varepsilon_o\varepsilon_\infty}{\Delta t^2} + \dfrac{\varepsilon_o\varepsilon_s\omega_o^2}{2}\right)}$$

$$+ s^n\frac{\left(\dfrac{2\varepsilon_o\varepsilon_\infty}{\Delta t^2}\right)}{\left(\dfrac{\varepsilon_o\varepsilon_\infty\delta}{\Delta t} + \dfrac{\varepsilon_o\varepsilon_\infty}{\Delta t^2} + \dfrac{\varepsilon_o\varepsilon_s\omega_o^2}{2}\right)} + f^{(n)2}\frac{\left(\dfrac{2\varepsilon_o\chi^{(2)}}{\Delta t^2}\right)}{\left(\dfrac{\varepsilon_o\varepsilon_\infty\delta}{\Delta t} + \dfrac{\varepsilon_o\varepsilon_\infty}{\Delta t^2} + \dfrac{\varepsilon_o\varepsilon_s\omega_o^2}{2}\right)}$$

$$+ f^{(n-1)2}\frac{\left(\dfrac{\varepsilon_o\chi^{(2)}\delta}{\Delta t} - \dfrac{\varepsilon_o\chi^{(2)}}{\Delta t^2} - \dfrac{\varepsilon_o\chi^{(2)}\omega_o^2}{2}\right)}{\left(\dfrac{\varepsilon_o\varepsilon_\infty\delta}{\Delta t} + \dfrac{\varepsilon_o\varepsilon_\infty}{\Delta t^2} + \dfrac{\varepsilon_o\varepsilon_s\omega_o^2}{2}\right)}$$

$$+ f^{(n+1)2}\frac{\left(\dfrac{-\varepsilon_o\chi^{(2)}\delta}{\Delta t} - \dfrac{\varepsilon_o\chi^{(2)}}{\Delta t^2} - \dfrac{\varepsilon_o\chi^{(2)}\omega_o^2}{2}\right)}{\left(\dfrac{\varepsilon_o\varepsilon_\infty\delta}{\Delta t} + \dfrac{\varepsilon_o\varepsilon_\infty}{\Delta t^2} + \dfrac{\varepsilon_o\varepsilon_s\omega_o^2}{2}\right)} \tag{12}$$

The above equation may be simplified into the following form.

$$s^{n+1} = \alpha_1 + \alpha_2 f^{(n+1)2} \tag{13}$$

where, α_1 and α_2 are obtained from the equation parameters. Similarly for the fundamental field, the FDTD approximation of Eq. (6) is as follows

$$\frac{\omega_o^2}{2}(D^{f(n+1)} + D^{f(n-1)}) + \frac{2\delta}{2\Delta t}(D^{f(n+1)} - D^{f(n-1)})$$

$$+ \frac{1}{\Delta t^2}(D^{f(n+1)} - 2D^{fn} + D^{f(n-1)}) = \frac{2\varepsilon_o\varepsilon_\infty\delta}{2\Delta t}(f^{n+1} - f^{n-1})$$

$$+ \frac{\varepsilon_o\varepsilon_\infty}{\Delta t^2}(f^{n+1} - 2f^n + f^{n-1}) + \frac{\varepsilon_o\varepsilon_s\omega_o^2}{2}(f^{n+1} + f^{n-1})$$

$$+ \frac{\varepsilon_o\chi^{(2)}\omega_o^2}{2}(f^{n+1}s^{n+1} + f^{n-1}s^{n-1})$$

$$+$$

$$+ \frac{\varepsilon_o\chi^{(2)}}{\Delta t^2}(f^{n+1}s^{n+1} - 2f^n s^n + f^{n-1}s^{n-1})$$

$$+ \frac{2\varepsilon_o\chi^{(2)}\delta}{2\Delta t}(f^{n+1}s^{n+1} - f^{n-1}s^{n-1}) \tag{14}$$

By substituting for s^{n+1} from Eq. (13) and rearranging, Eq. (14) becomes in the form

$$f^{(n+1)3} + af^{(n+1)2} + bf^{n+1} + c = 0 \tag{15}$$

which is a cubic polynomial in f^{n+1} with

$a = 0$,

$$b = \frac{\varepsilon_o\varepsilon_\infty\delta}{\Delta t} + \frac{\varepsilon_o\varepsilon_\infty}{\Delta t^2} + \frac{\varepsilon_o\varepsilon_s\omega_o^2}{2} + \frac{\alpha_1\varepsilon_o\chi^{(2)}\omega_o^2}{2} + \frac{\alpha_1\varepsilon_o\chi^{(2)}\delta}{\Delta t} + \frac{\alpha_1\epsilon_o\chi^{(2)}}{\Delta t^2}$$

and

$$c = f^n\left(-\frac{2\varepsilon_o\varepsilon_\infty}{\Delta t^2} - \frac{2\varepsilon_o\chi^{(2)}s^n}{\Delta t^2}\right)$$

$$+ f^{n-1}\left(\frac{-\varepsilon_o\varepsilon_\infty\delta}{\Delta t} + \frac{\varepsilon_o\varepsilon_\infty}{\Delta t^2} + \frac{\varepsilon_o\varepsilon_s\omega_o^2}{2} + \frac{\varepsilon_o\chi^{(2)}\omega_o^2 s^{n-1}}{2}\right)$$
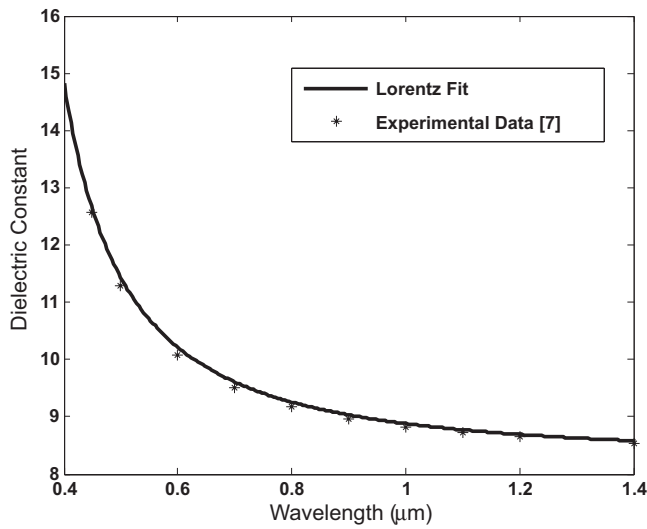
Figure 1 The material dispersion relation. Solid lines: Lorentz fit, *: experimental data [7]

$$-\frac{\varepsilon_o\chi^{(2)}\delta s^{n-1}}{\Delta t} + \frac{\varepsilon_o\chi^{(2)}s^{n-1}}{\Delta t^2}\right) - D^{f(n+1)}\left(\frac{\omega_o^2}{2} + \frac{\delta}{\Delta t} + \frac{1}{\Delta t^2}\right)$$

$$+ D^{fn}\left(\frac{2}{\Delta t^2}\right) - D^{f(n-1)}\left(\frac{\omega_o^2}{2} - \frac{\delta}{\Delta t} + \frac{1}{\Delta t^2}\right)$$

For the range of values used in SHG problems, only one solution is found to be physical and is given by

$$f^{n+1} = -2\sqrt{Q}\cos\left(\frac{\theta}{3}\right) - \frac{a}{3} \tag{16}$$

where, $Q = \frac{a^2 - 3b}{9}$, $R = \frac{2a^3 - 9ab + 27c}{54}$ and $\theta = \arccos(R/\sqrt{Q^3})$.

The update equations for the flux densities of the fundamental and second harmonic waves are given by the following FDTD equations.

$$D^{f(n+1)} = 2D^{f(n)} - D^{f(n-1)} + \frac{\Delta t^2 \nabla^2 f^n}{\mu} \tag{17}$$

$$D^{s(n+1)} = 2D^{s(n)} - D^{s(n-1)} + \frac{\Delta t^2 \nabla^2 s^n}{\mu} \tag{18}$$

4. RESULTS AND ANALYSIS

The resulting FDTD scheme is fully explicit. The algorithm starts by first finding all D^{n+1} components using Eq. (17) and (18). To calculate the value of f^{n+1}, only the coefficient c in Eq. (15) needs to be updated every time step. Once the quantity f^{n+1} is found, s^{n+1} is calculated according to Eq. (13). For very strong input pump levels, the stability condition becomes slightly less than the linear case.

To study the effectiveness of the proposed FDTD scheme, a homogeneous AlGaAs structure is considered. The dispersion relation of the material is obtained from published experimental data [7] and fitted to Lorentz model of Eq. (3). With $\varepsilon_\infty = 1.24$, $\varepsilon_s = 2.88$, $\omega_o = 0.65 \times 10^{16}$ rad/s, and $\delta = 6.0 \times 10^{13}$ rad/s, a very good agreement is achieved, as shown in Figure 1. The nonlinear susceptibility is taken as $\chi^{(2)} = 113$ pm/V. A Gaussian pulse excitation with 30 fs waist at a fundamental wavelength of $\lambda_f =$

1.064 μm and maximum amplitude of $A = 100$ V/μm is applied. The transverse profile of this excitation is also Gaussian with a spot size of 5 μm.

The FDTD mesh parameters are set such that stability with minimum possible numerical dispersion is insured. It is very essential that the numerical dispersion does not plague the physical dispersion. Hence, a fourth-order accurate FDTD approximation for the spatial derivatives in Eqs. (17) and (18) is used. It has been shown that such a scheme significantly improves the accuracy and efficiency of the solution [8]. The mesh size in the transverse direction is $\Delta x = \lambda_f/10$ and in the propagation direction is $\Delta y = \lambda_f/100$. Absorbing boundary conditions cover all sides of the computational domain. The algorithm is tested for two cases: SHG using selective-dispersion and using full dispersion. In the selective- dispersion case, ε_r^f and ε_r^s in Eqs (1) and (2) are not taken as continuous functions of frequency. Instead, each is assigned a constant value according to the dispersion relation of Figure 1 at $\lambda_f = 1.064$ μm and $\lambda_s = 0.532$ μm, respectively, as in Ref. 9.

For dispersive materials, the amount of power exchange in the second harmonic generation process is a strong function of phase shift between the propagating waves. This phase shift is defined by the refractive indexes values associated with each frequency component of the coexisting waves, as given by the dispersion relation. Figure 2 shows the propagation of the input fundamental pulse (30-fs waist) and the subsequent generation of the second harmonic pulse along the structure. The profile of the two pulses is drawn at the midpoint in the transverse direction. At the onset of the introduction of the input pulse, the nonlinearity of the material is excited and a new pulse at double the input frequency starts to develop. Because of the difference in central (carrier) frequency between the two pulses, each will travel at its own group velocity. The fundamental pulse moves at a higher group velocity than the second harmonic pulse. Eventually, the fundamental pulse by-passes the second harmonic pulse and the interaction between the two pulses stops. Further, the second harmonic pulse suffers severe distortion and eventually it breaks up. The higher frequency terms travel at a slower velocity, whereas the low frequency components travel closer to the fundamental velocity. A three dimensional representation of the propagation of the two pulses is shown in Figure 3.

The simulated power curves of this case are shown in Figure 4. Due to group velocity mismatch (GVM) phenomenon, the power
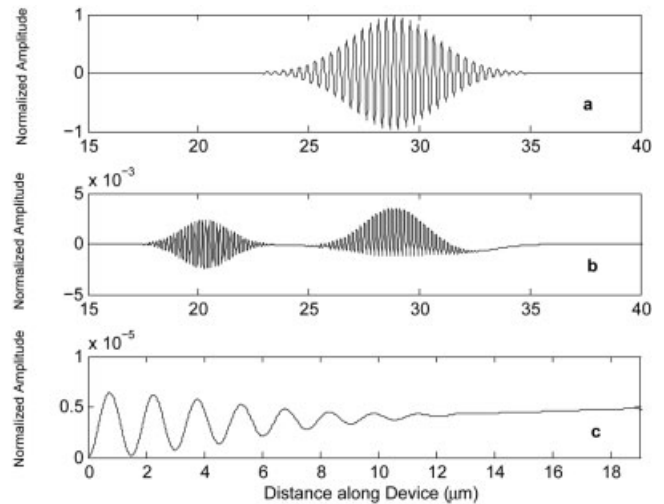

Figure 2 The fundamental and the second harmonic pulse profiles along the nonlinear dispersive medium at the end of simulation time
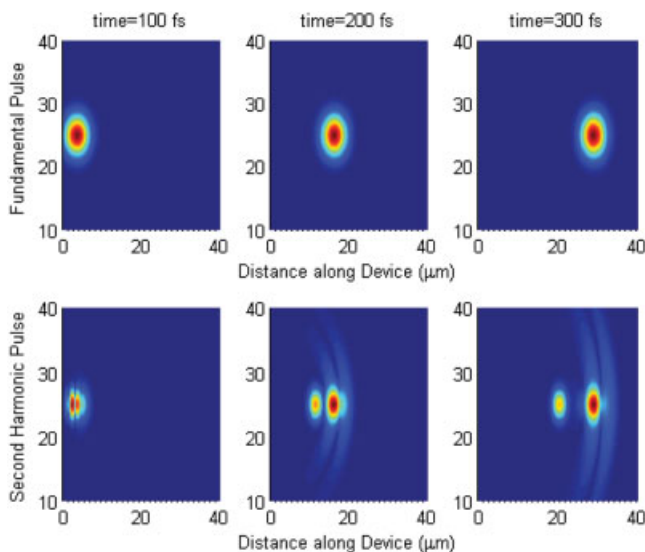
Figure 3 A three dimensional representation of the propagation of the fundamental and second harmonic pulses inside the dispersive structure. [Color figure can be viewed in the online issue, which is available at www.interscience.wiley.com]

exchange between the propagating input pulse and the generated SH pulse diminishes along the propagation direction. Eventually, the two pulses seize to interact. The power exchange for the CW case [5] is shown in Figure 4 (thin line), for comparison. It should be pointed out here that selective dispersion is not a valid approximation of the dispersion relation at ultrashort optical pulse conditions, as shown in Figure 4 (dotted line).

5. CONCLUSIONS

The effect of material dispersion on the efficiency of pulsed second harmonic generation in optical structures containing second order nonlinearities is presented. The frequency-dependent material response is incorporated into the time-domain model using the ADE approach. Further, a decoupled FDTD solution algorithm equipped with 4th order spatial approximations has been formulated. The
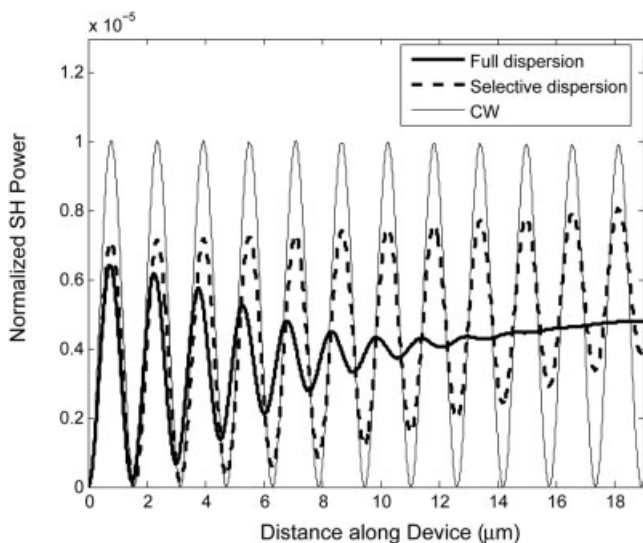

Figure 4 Normalized second harmonic power along the nonlinear medium with full dispersion and selective dispersion when compared with the CW case

application of this FDTD algorithm for modeling short-pulse SHG in dispersive nonlinear optical material has been demonstrated. Numerical results for the generated second harmonic pulse clearly demonstrate the pulse break-up phenomenon.

REFERENCES

1. M. Fejer, G. Magel, D. Jundt, and R. Byer, Quasi-phase matched second harmonic generation: Tuning and tolerance, IEEE J Quantum Electron 28 (1992), 2631–2654.
2. I. Tomov, R. Fedosejevs, and A. Offenberger, Up-conversion of sub-picosecond light pulses, IEEE J Quantum Electron 18 (1982), 2048–2056.
3. E. Sidick, A. Knosen, and A. Dienes, Ultrashort-pulse second-harmonic generation. I. Transform-limited fundamental pulses, J Opt Soc Am B 12 (1995), 1704–1712.
4. A. D'Orazlo, D. de ceglia, M. De Sario, V. Petruzzelli, and F. Prudenzano, Second order nonlinear interactions in periodic waveguides, ICTON 1 (2004), 126–130.
5. M.A. Alsunaidi, H.M. Masoudi, and J.M. Arnold, A time-domain algorithm for second harmonic generation in nonlinear optical structures, IEEE Photonics Tech Lett 12 (2000), 395–397.
6. A. Taflove, Computational electrodynamics: The finite-difference time-domain method. Artech House, Norwood, MA, 1995.
7. S. Gehrsitz, F.K. Reinhart, C. Gourgon, N. Herres, A. Vonlanthen, and H. Sigg, The refractive index of $Al_xGa_{1-x}As$ below the band gap: Accurate determination and empirical modeling, J Appl Phys 87 (2000), 7825–7837.
8. M.A. Alsunaidi and F. Al-Hajiri, A higher-order accurate FDTD solution to scalar SHG problems, Proceedings of PIERS 2007, Prague, Czech Republic, 2007, pp. 475–478.
9. H. Masoudi, A time-domain beam propagation method for analyzing pulsed optical beams in second order nonlinear waveguides, Microwave Opt Technol Lett 28 (2001), 253–257.

APERTURE-COUPLED CIRCULARLY POLARIZED F-SLOT MICROSTRIP ANTENNA

Yong Yeh,[1] Nasimuddin,[2] Z. N. Chen,[2] and A. Alphones[1]
[1] School of EEE, Nanyang Technological University, Singapore 639798, Singapore
[2] RF and Optical Department, Institute for Infocomm Research, 1 Fusionopolis Way, #21–01 Connexis, Singapore 138632, Singapore; Corresponding author: nasimuddin@i2r.a-star.edu.sg

ABSTRACT: *A compact, aperture-coupled, circularly polarized F-slot microstrip antenna is proposed. The F-slot is embedded in the square microstrip patch and fed using an aperture-coupled feeding structure. The proposed antenna has a 4.87% (2.40–2.52 GHz) 3 dB AR (axial ratio) bandwidth with a 14.4% 10 dB return loss bandwidth. The gain within the usable bandwidth remains relatively constant at 6.0 dBic with a ±0.5 dB variation and a peak gain is 6.2 dBic at 2.42 GHz. The antenna ground plane size and foam substrate thickness represent about 53.3 and 7% of its wavelength at the operating frequency of 2.46 GHz, respectively. The 3 dB AR beamwidth is >90°. The patch size of the proposed antenna is reduced by 22.7% compared with a conventional*